Atmos. Chem. Phys. Discuss., 9, 18965–18984, 2009
www.atmos-chem-phys-discuss.net/9/18965/2009/

Atmospheric Chemistry and Physics Discussions

This discussion paper is/has been under review for the journal *Atmospheric Chemistry and Physics (ACP)*. Please refer to the corresponding final paper in *ACP* if available.

Measurements of coarse mode and primary biological aerosol transmission through a tropical forest canopy using a dual-channel fluorescence aerosol spectrometer

A. M. Gabey, M. W. Gallagher, J. Whitehead, and J. Dorsey

Centre for Atmospheric Science, University of Manchester, Manchester M13 9PL, UK

Received: 25 August 2009 – Accepted: 29 August 2009 – Published: 11 September 2009

Correspondence to: A. M. Gabey (andrew.m.gabey@postgrad.manchester.ac.uk)

Published by Copernicus Publications on behalf of the European Geosciences Union.

Abstract

Aerosol in the size range 0.8–20 μm was characterized according to optical equivalent diameter, D_P, morphology and the presence of biological material, the latter determined by recording fluorescence excited by ultraviolet light pulses at two different wavelengths. Single-particle measurements were performed within and subsequently above a tropical rainforest in Borneo, Malaysia, in June and July 2008. In both locations the aerosol number size distribution exhibited a primary biological aerosol (PBA) mode sized 2 μm$<D_P<$20 μm and much larger in number within the forest than above it, suggesting the PBA originates below the canopy. PBA was observed to dominate the total number at $D_P>2$ μm and possessed a wider morphological range than non-PBA. It also accounted for around 80% of the total number in the understory and 40% of the total number above canopy. Canopy transmission efficiencies for the total aerosol number and PBA are calculated to be 0.48±0.19 and 0.31±0.15 respectively, with the former appearing to peak during the daytime because of a lack of PBA emission below the canopy.

1 Introduction

A Primary Biological Aerosol (PBA) particle is defined as an aerosol particle that is discernibly all or part of a living organism. The classification includes pollen, animal and plant fragments, bacteria, viruses and fungal spores. The ubiquity of PBA, particularly fungal spores and pollen, in the atmosphere (e.g. Jaenicke and Matthias-Maser, 1993) has led to a renewed interest in aerobiology in the past 15 years. The fraction swept into cloud-forming regions of the atmosphere by updraughts can reside in the atmosphere for weeks and travel up to 1000 km. It is here that much of the current research interest is focussed, since pollen have been observed to initiate cloud droplet freezing at temperatures around 4°C warmer than non-PBA in the laboratory (Diehl et al., 2001, 2002). PBA number concentration in cloud-forming regions is ~5 L^{-1}, which

ACPD

9, 18965–18984, 2009

approximately matches that of ice nuclei (Matthias-Maser et al., 1999), yet their wider impact on cloud processes is not well quantified.

Fungi thrive in dark, warm and damp environments with abundant soil nutrients or plant life. The lower strata of tropical forests are home to a high density of fungi (Lowman, 2004). Traditional biological sampling techniques used in and below tropical canopies (Gilbert, 2005) show the spore number concentration to be larger at the ground than in the upper canopy. The canopy itself can be regarded as a sink for vertically transported material, inhibiting its transfer to the free atmosphere. After nightfall, an upward heat flux typically occurs below the canopy as its top cools radiatively with warm air is trapped beneath (e.g. Kruijt et al., 2000). This suppresses the mixing of air through the canopy and therefore also the transport of aerosol. The net effect is that particles are channelled below the canopy until they reach a clearing large enough to allow their escape.

Tropical forests are estimated to cover 1090–1220 million hectares in total (Mayaux et al., 1998), representing a widespread PBA source. A first global estimate of the total fungal spore emission rate was placed at ~50 Tg/yr by Elbert et al., 2007, so measuring the degree to which the canopy impedes PBA transport into the free atmosphere is a logical first step in bridging the gulf between the predicted and observed atmospheric PBA loadings. We present time-resolved measurements of a S.E. Asian tropical rainforest canopy's average particle transmission efficiency for PBA and total aerosol in an optical diameter range of 0.8–20 μm. Data was collected using a novel bio-aerosol spectrometer, the Wide Issue Bioaerosol Spectrometer, version 3 (WIBS-3), at the forest floor and above the canopy. Information about relative humidity (RH) and temperature (T) at these positions is also included to illustrate the contrast between the wider area and the microclimate of the forest understory.

ACPD
9, 18965–18984, 2009

2 Location of measurements

The measurement site was located in Danum Valley, a Conservation area of tropical rainforest in Malaysian Borneo established in 1981. Measurements were based at a ridge, Bukit Atur, as part of the Aerosol Coupling in the Earth System (ACES) and the Oxidant, Particulate and Photochemical Processes (OP3) field campaigns in 2008 (Hewitt, 2009). The below-canopy site was located at the sloping base of the ridge at 196 m a.s.l. The above-canopy measurement site was located atop the ridge at 04°58′53″ N 117°50′37″ E, 426 m a.s.l., overlooking the below-canopy site which was approximately 1 km away. The WIBS-3 inlet was located 2 m above the forest floor in the understory and subsequently ∼12 m above the canopy, which propagated up the hillside.

Danum Valley is situated in the Yayasan Sabah Forestry Division, located in the Sabah Federal State of Malaysia. The conservation area is 43 800 Ha, representing 4.5 percent of the 972 804 Ha New Yayasan Sabah Concession Area (NYSCA), which is currently unlogged (Marsh and Greer, 1992). The forest in Danum Valley is categorised as a tropical lowland evergreen rainforest and has an estimated average height of 35 m at the below-canopy measurement site. The valley receives an annual mean rainfall of 2778 mm (Fook, Malaysia Meteorological Dept., private communication, 2007) and April is the driest month (159 mm). Sunrise and sunset times were 06:00 and 18:15 LT respectively.

PBA and meteorological measurements were conducted in forest understory and above the canopy in two phases: 16 April–3 May and 19 June–23 July 2008, with 580 hours of data collected in total. Above-canopy WIBS-3 data was only collected in July, therefore this analysis and discussion is based solely on the second measurement phase in order to reduce uncertainty arising from month-to-month changes in conditions. The absolute vertical separation of the sites is ∼200 m. Data from the WIBS-3 was recorded for 14 full days below canopy and 2.2 days of continuous data were collected above canopy.

ACPD
9, 18965–18984, 2009

3 Instrumentation used

3.1 Particle measurements

Coarse mode aerosol number concentration, morphology and fluorescence (used to indicate PBA) were sampled using the WIBS-3: a single particle, dual-wavelength UV fluorescence spectrometer, (Kaye et al., 2005). The instrument operates by exciting single particles sequentially, using two ultra-violet pulses at 280 nm and 370 nm, selected to excite primarily the co-enzyme NADH and the amino acid Tryptophan. Two detectors, tuned to the emission bands of Tryptophan and NADH (310–400 nm and 400–600 nm respectively), record the intensity of any fluorescence induced by the UV pulses.

Particles with optical equivalent diameter (D_P) 0.5–20 μm are sized using Mie scattering. Each particle passes through a laser beam and the elastically scattered light is focussed onto a quadrant PMT that samples its intensity at four points. The summed intensity is used to calculate optical size and the fractional standard deviation between the quadrants parameterises particle morphology; a low standard deviation indicates a more symmetrical scattering pattern, normally produced by a spherical particle. This morphological parameter is known as the Asymmetry Factor, *AF*, whose distribution is intrinsically log-normal.

The particle number concentration measured by WIBS-3 was confirmed in-situ by comparison against a commercial optical particle counter (GRIMM Dust Monitor Model 1.108) co-located with the WIBS-3 in the understory.

3.2 Meteorological measurements

Absolute temperature (T) and relative humidity (RH) were measured in the understory using a warmed probe for improved accuracy in near condensing environments (Vaisala Model HMT 337 consisting of a PT100 RTD sensor, range −70 to +180°C, accuracy ±0.2°C at 20°C, and a HUMICAP© 180R sensor for humidity, range 0 to 100%

ACPD
9, 18965–18984, 2009

RH, accuracy ±1.0% from 0 to 90% and ±1.7% from 90 to 100%).

4 Methods

It was assumed that PBA are the only fluorescent aerosol in the coarse mode and that to be recorded as such, their fluorescence must exceed an instrument-defined minimum threshold in either channel. The measured PBA concentration is therefore a subset of the total measured concentration. A similar protocol has been employed with other UV bioaerosol spectrometers (e.g. Agranovski and Ristovski, 2005). Random noise from UV pulse intensity fluctuations, component fluorescence and electrical noise is estimated to cause an over-estimate of PBA number that is 2–3% of the total measured number because of non-fluorescent particles being misclassified as fluorescent in either channel.

To calculate diurnal averaged time series, data of 5-min time resolution was separated according to the half-hour of the day in which it occurred and averaged across the whole dataset. Simultaneous monitoring above and below the canopy was not possible, so the canopy transfer efficiencies were calculated by taking the continuous above-canopy data and dividing it by a time series generated by replicating the diurnal average of the below-canopy data. The resulting time series of transfer efficiencies was diurnally averaged to illustrate its apparent dependence on time of day.

5 Results and discussion

5.1 Temperature and humidity

Figures 1 and 2 display the average diurnal cycles of RH and T above and below the canopy. Relatively small standard deviations (bars) in the below-canopy plots indicate the variation of T and RH is suppressed because the canopy shields the site from incoming solar radiation, prevents efficient exchange of moist and dry air and acts as

ACPD
9, 18965–18984, 2009

a thermal insulator at night. The result is a highly consistent diurnal cycle of both variables. Above the canopy both exhibit a larger dynamic range and RH is usually lower because of less inhibited turbulent exchange outside the canopy.

5.1.1 Particle concentration below the canopy

A strong diurnal cycle of coarse aerosol number is observed in the understory. Figure 3 shows the total WIBS-3 number concentration for $0.8\,\mu m < D_P < 20\,\mu m$, N_{TW}, for one characteristic week. PBA number, N_{PBA}, clearly dominates the variation of N_{TW} and initially peaks at 15:00 LT. A sustained series of bursts maintains a concentration of ~1500–2000 L^{-1} following sunset, ceasing before sunrise and giving rise to concentrations ~300 L^{-1}. Aerosol removal by rain washout appears to be mitigated by interception and channelling of rainwater by the canopy.

The average diurnal cycle of N_{TW} is displayed in Fig. 4(i), which shows N_{TW} to be consistently smaller in the daytime than it is between 15:00 LT and sunrise. Comparing the diurnally averaged N_{PBA} number, printed in Fig. 4(ii), with the corresponding RH plot in

Figure 1 (lower panel) suggests that PBA release and the recovery in RH both occur at 15:00 LT, signifying a possible link. The nature of the emission process is thought to be fungal spore release triggered by raised relative humidity and this will be discussed in detail in a forthcoming paper.

5.1.2 Particle concentration above canopy

Above the canopy, N_{PBA} is reduced to around one-quarter of its mean below-canopy value, from 1200 L^{-1} to 300 L^{-1}, and there is no evidence of the understory's diurnal cycle occurring here. Fig. 5 depicts the time series of N_{TW} and N_{PBA}. N_{PBA} does not appear to exhibit any clear diurnal pattern above the canopy. Non-PBA concentration ($N_{NON} = N_{TW} - N_{PBA}$) is somewhat enhanced compared to the understory. Short-term fluctuations are driven by rain washout, as observed around 18:00 LT on July 19. The

ACPD
9, 18965–18984, 2009

difference between the plots in Fig. 5 represents the non-biological aerosol component, $N_{NON,}$ which takes around 2 h to reassert itself compared to the rapid recovery in N_{PBA}.

5.2 Comparison of total and PBA size distributions in each location

Mean number size distributions ($dN/d\log Dp$) were calculated for (i) all particles and (ii) the biological and non-biological components separately. The respective distributions are shown in Figure 6(i) and (ii), in above and below canopy pairs. Each of the three plots exhibits similar size modes above and below the canopy, albeit with different absolute concentrations. The mode at around 1 μm, present only in Fig. 6(i), is enhanced from 300 to 500 L^{-1} above the canopy and the 2 $\mu m < D_P < 5\,\mu m$ peak concentration reduces from ~80 L^{-1} below canopy to ~200 L^{-1} above it. The PBA and non-PBA distributions shown in Fig. 6 (ii) exclusively contain different size modes, suggesting the ~1 μm mode is a different species and, because of its strengthened presence above the canopy, it may originate outside the forest.

5.3 Comparison of asymmetry factor distributions in each location

In order to compare the morphological properties of the two size modes, *AF* data was split into several size bands. This process was performed for above and below-canopy data and their frequency distributions, each normalised to its own maximum, are plotted in Fig. 7(i) and (ii). In the understory distributions, the *AF* mode lies at 5 for $D_P \leq 2\,\mu m$ and for bigger particles a systematic shift to an *AF* mode at 11 takes place. Above canopy the same modes appear but the transition to the high-*AF* regime is not complete until the 4–6 μm size range is reached. The gradual transition takes place because the PBA and non-PBA size distributions overlap at $2 < D_P < 4\,\mu m$ but neither species dominates the total number in this size range above the canopy.

ACPD
9, 18965–18984, 2009

5.4 Canopy transmission

Diurnal average canopy transmission efficiencies at 30-min time resolution were calculated using the WIBS data for (i) all particles sized 0.8–20 μm and (ii) those suspected to be PBA and these are shown in Fig. 8(i) and (ii). The error bars show standard deviation, a characteristic of the day-to-day variation in above-canopy number concentration, which as a proportion of the total concentration is far larger than below the canopy where a more consistent diurnal cycle occurs. Mean daytime, night-time and whole day transmission efficiencies for PBA, E_{PBA}, and total number, E_{TW}, are displayed in Table 1.

In both Fig. 8 (i) and (ii), there is a clear minimum at 14:00 and a maximum at 09:00 h, indicating the transition between the daytime and night-time regimes. The overall mean E_{TW} exceeds the corresponding E_{PBA} because of the reduced N_{PBA} and enhanced N_{NON} above the canopy.

6 Conclusions

The recorded *AF*, PBA and total number size spectra all contain the same features above and below the canopy, suggesting that the coarse aerosol sampled at each height is from the same source. Above the canopy the significantly reduced abundance of PBA, which dominates the total number of particles larger than 2 μm, is consistent with production below and transmission through the canopy with a finite efficiency. The 1 μm $d\mathrm{N}/d\log D_P$ mode has a negligible fluorescent component, likely attributable to it being a different species to the larger size mode rather than a lack of fluorescence sensitivity to smaller fluorescent particles. This conclusion is reinforced by the contrasting *AF* distributions at these sizes, which show modally lower *AF* than for larger particles. These findings are contrary to laboratory tests using the WIBS-3 using polystyrene latex (PSL) spheres. Modal *AF* actually rose by 2–3 (arbitrary units) when 3 μm PSL spheres were substituted with 1 μm PSL spheres, ruling out the possibility that instru-

ACPD
9, 18965–18984, 2009

ment artefacts dominate the tropical *AF* measurements.

The above-canopy time series of concentration according to the WIBS-3 features nothing to suggest sustained periods of exchange at a particular time of day. The diurnal cycles of derived canopy transmission efficiency, printed in Fig. 8, are primarily influenced by the changes in concentration in the understory. What on first inspection appears to be a period of enhanced particle transmission around local midday is in fact the period during which the understory concentration is at its minimum, although enhanced transport could also conceivably occur at this time of day, when PBA emissions are at their weakest. The mid-afternoon minima in the transmission efficiency plots appear because of the initiation of the below-canopy PBA emission mechanism re-starting, thereby increasing the relative number below canopy. Since a channelling of aerosol beneath the canopy is expected, it is unclear whether the large differences between above-canopy concentrations during the two-day dataset are dictated by direct transmission through the canopy or the cumulative effect of forest clearings in the surrounding area.

References

Agranovski, V. and Ristovski, Z. D.: Real-time monitoring of viable bioaerosols: capability of the UVAPS to predict the amount of individual microorganisms in aerosol particles, J. Aerosol Sci., 36, 665–676, 2005.

Diehl, K., Quick, C., Matthias-Maser, S., Mitra, S. K., and Jaenicke, R.: The ice nucleating ability of pollen Part I: Laboratory studies in deposition and condensation freezing modes, J. ATMOS RES, 75–87, 2001.

Diehl, K., Quick, C., Matthias-Maser, S., Mitra, S. K., and jaenicke, R.: The ice nucleating ability of pollen Part II: Laboratory studies in immersion and contact freezing modes, J. Atmos. Res., 75–87, 2002.

Elbert, W., Taylor, P. E., Andreae, M. O., and Pöschl, U.: Contribution of fungi to primary biogenic aerosols in the atmosphere: wet and dry discharged spores, carbohydrates, and

ACPD

9, 18965–18984, 2009

inorganic ions, Atmos. Chem. Phys., 7, 4569–4588, 2007, http://www.atmos-chem-phys.net/7/4569/2007/.
Gilbert, G. S. and Reynolds, D. R.: Nocturnal Fungi: Airborne Spores in the Canopy and Understory of a Tropical Rain Forest, Biotropica, 37, 462–464, 2005.
Hewitt, C. N., Lee, J., Barkley, M. P., Chappell, N. A., Coe, H., Collier, C., Commane, R., DiCarlo, P., Edwards, P. M., Evans, M. J., Furneaux, K. L., Gallagher, M., Guenther, A., Heard, D. E., Ingham, T., Irwin, M., Langford, B., Lim, S. F., MacDonald, S., MacKenzie, A. R., Mahajan, A., McFiggans, G., Mills, G., Misztal, P., Monks, P. S., Nemitz, E., Nicolas-Perea, V., Oetjen, H., Oram, D., Palmer, P. I., Plane, J. M. C., Pyle, J. A., Reeves, C. E., Robinson, N. H., Stewart, D., Stone, D., and Whalley, L. K.: Oxidant and particle photochemical processes above a south-east Asian tropical rain forest (the OP3 project): rationale, location characteristics, tools and overview, submitted to Atmos. Chem. Phys. Discuss., 2009.
Jaenicke, R. and Matthias-Maser, S.: The direct contribution of the biosphere to the atmospheric aerosol, Aerosol Sci., 24, 537–538, 1993.
Kaye, P. H., Stanley, W. R., and Hirst, E.: Single particle multichannel bio-aerosol fluorescence sensor, Optics Express, 13, 3583–3593, 2005.
Kruijt, B., Malhi, Y., Lloyd, J., Norbre, A. D., Miranda, A. C., Pereira, M. G. P., Culf, A., and Grace, J.: Turbulence Statistics Above And Within Two Amazon Rain Forest Canopies, Bound.-Lay. Meteorol., 94, 297–331, 2000.
Lowman, M. and Rinker, H. B.: Forest canopies, 2 ed., Academic Press, 2004.
Marsh, C. W. and Greer, A. G.: Forest Land-Use in Sabah, Malaysia – an Introduction to Danum Valley, Philosophical Transactions of the Royal Society of London Series B-Biological Sciences, 335, 331–339, 1992.
Matthias-Maser, S., Reichert, K., and Jaenicke, R.: Primary Biological Aerosol Particles at the High Alpine Site of Jungfraujoch/Switzerland, Aerosol Sci., 31, 955–956, 1999.
Mayaux, P., Achard, F. R., and Malingreau, J.-P.: Global tropical forest area measurements derived from coarse resolution satellite imagery: a comparison with other approaches, Environ. Conser., 25, 37–52, 1998.

ACPD
9, 18965–18984, 2009

Table 1. Summary of tropical forest canopy transmission efficiencies of all particles and primary biological aerosol particles identified by the WIBS-3 and broken down by time of day.

Canopy transmission efficiencies	
All particles $0.8<D_P<20\,\mu m$	Mean transmission efficiency
OVERALL	0.58±0.27
NIGHT	0.48±0.19
DAY	0.83±0.28
PBA $0.8<D_P<20\,\mu m$	
OVERALL	0.31±0.15
NIGHT	0.38±0.15
DAY	0.29±0.12

ACPD
9, 18965–18984, 2009

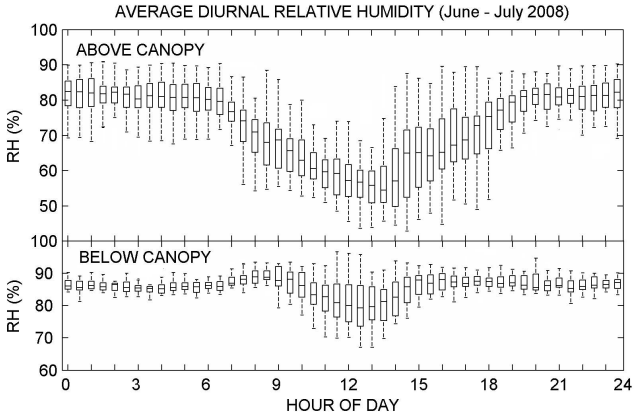

Fig. 1. Half-hourly average relative humidity over the measurement period above the forest canopy (upper panel) and 2 m above the forest floor (lower panel).

ACPD

9, 18965–18984, 2009

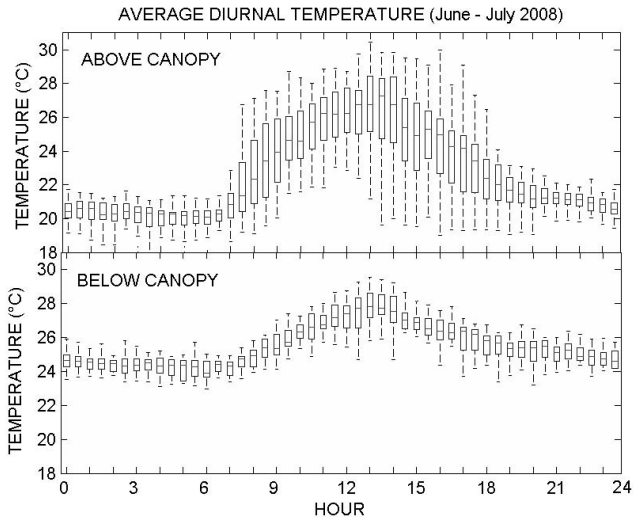

Fig. 2. Half-hourly mean air temperature for the measurement period above the forest canopy (upper panel) and 2 m above the forest floor (lower panel).

ACPD
9, 18965–18984, 2009

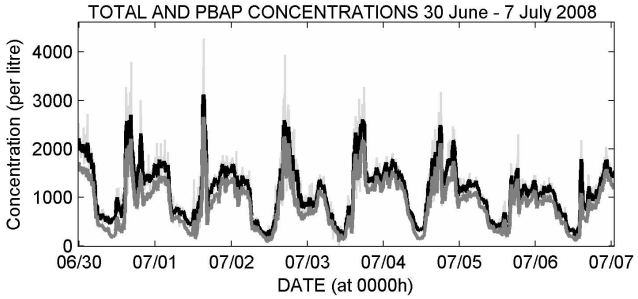

Fig. 3. One representative week of below-canopy coarse aerosol number (black line) and coarse PBA number according to the WIBS-3 (grey line). Date ticks represent local midnight.

ACPD
9, 18965–18984, 2009

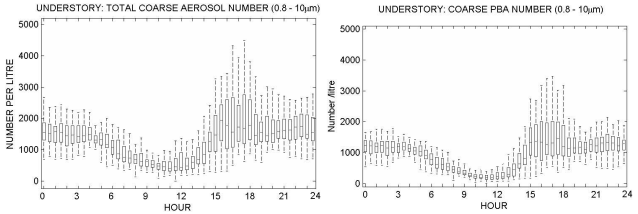

Fig. 4. Box-and-whisker plots representing the diurnal average concentration of (i) all aerosol sized 0.8–20 μm and (ii) all aerosol classed as PBA.

ACPD

9, 18965–18984, 2009

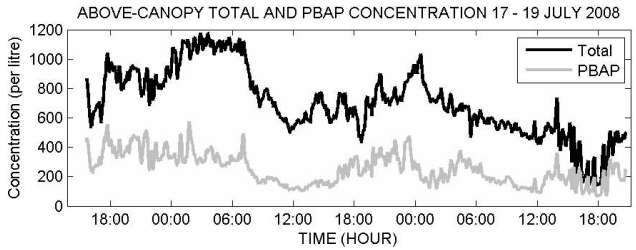

Fig. 5. Time series of Total and PBA aerosol number concentration above canopy.

ACPD
9, 18965–18984, 2009

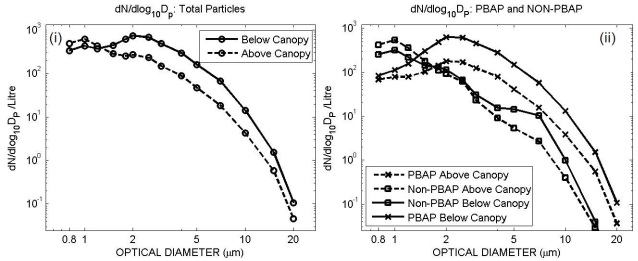

Fig. 6. Mean number size distributions of (i) all aerosol sized 0.8–20 μm and (ii) the PBA and non-PBA subpopulations according to the WIBS-3.

ACPD
9, 18965–18984, 2009

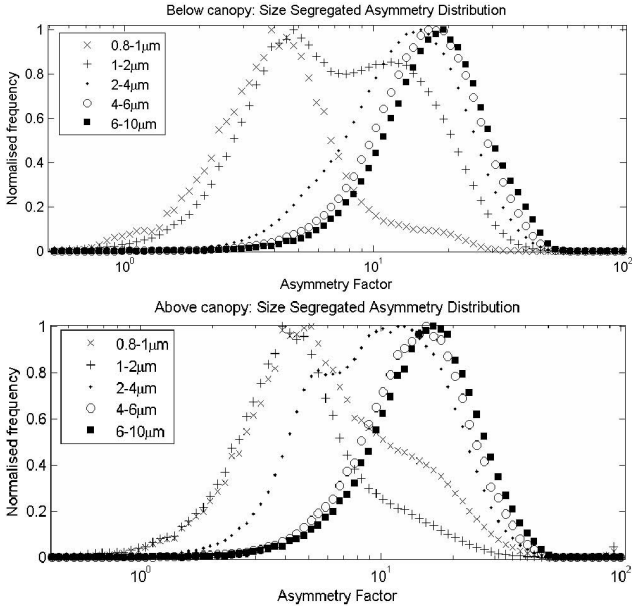

Fig. 7. Size-segregated asymmetry factor (AF) distributions at (i) below and (ii) above canopy sites. Each plot is normalised to the peak AF in each size range.

ACPD
9, 18965–18984, 2009

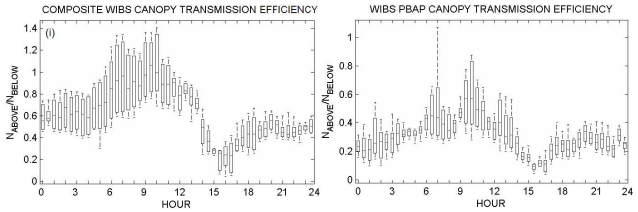

Fig. 8. Box and whisker plots showing diurnally averaged canopy transmission efficiency for (i) all particles and (ii) PBA, based on WIBS-3 measurements at different times.

ACPD

9, 18965–18984, 2009